Targeting of the N-terminal coiled coil oligomerization interface by a helix-2 peptide inhibits unmutated and imatinib-resistant BCR/ABL

ARTICLE *in* INTERNATIONAL JOURNAL OF CANCER · JUNE 2008

Impact Factor: 5.09 · DOI: 10.1002/ijc.23467 · Source: PubMed

7 AUTHORS, INCLUDING:

Tim Beissert
Goethe-Universität Frankfurt am Main
21 PUBLICATIONS **505** CITATIONS
SEE PROFILE

Lorena Travaglini
Ospedale Pediatrico Bambino Gesù
25 PUBLICATIONS **1,189** CITATIONS
SEE PROFILE

Afsar Ali Mian
Goethe-Universität Frankfurt am Main
14 PUBLICATIONS **82** CITATIONS
SEE PROFILE

Clara Nervi
Sapienza University of Rome
110 PUBLICATIONS **8,100** CITATIONS
SEE PROFILE

Int. J. Cancer: **122,** 2744–2752 (2008)

Targeting of the N-terminal coiled coil oligomerization interface by a helix-2 peptide inhibits unmutated and imatinib-resistant BCR/ABL

Tim Beissert[1]*, Alena Hundertmark[1], Velina Kaburova[1], Lorena Travaglini[2], Afsar A. Mian[1], Clara Nervi[2,3] and Martin Ruthardt[1]*

[1]*Med. Klinik II/Abt. Hämatologie, Johann Wolfgang Goethe-Universität, 60590 Frankfurt, Germany*
[2]*Dipartimento di Istologia ed Embriologia Medica, Universita "La Sapienza" Rome, Italy*
[3]*Institute of Cell Biology and Tissue Engineering, San Raffaele Bio-Medical Science Park of Rome, Rome, Italy*

The BCR/ABL oncogene is responsible for the phenotype of Philadelphia chromosome-positive (Ph+) leukemia. BCR/ABL exhibits an aberrant ABL-tyrosine kinase activity. The treatment of advanced Ph+ leukemia with selective ABL-kinase inhibitors such as Imatinib, Nilotinib and Dasatinib is initially effective but rapidly followed by resistance mainly because of specific mutations in BCR/ABL. Tetramerization of ABL through the N-terminal coiled-coil region (CC) of BCR is essential for the ABL-kinase activation. Targeting the CC-domain forces BCR/ABL into a monomeric conformation reduces its kinase activity and increases the sensitivity for Imatinib. We show that (*i*) targeting the tetramerization by a peptide representing the Helix-2 of the CC efficiently reduced the autophosphorylation of both unmutated and mutated BCR/ABL; (*ii*) Helix-2 inhibited the transformation potential of BCR/ABL independently of the presence of mutations; and (*iii*) Helix-2 efficiently cooperated with Imatinib as revealed by their effects on the transformation potential and the factor-independence related to BCR/ABL with the exception of mutant T315I. These findings support earlier observations that BCR/ABL harboring the T315I mutation have a transformation potential that is at least partially independent of its kinase activity. These data provide evidence that the inhibition of tetramerization inhibits BCR/ABL-mediated transformation and can contribute to overcome Imatinib-resistance.

Key words: Ph+ leukemia; BCR/ABL; oligomerization; molecular targeting; Imatinib-resistance

The major oncogene of Philadelphia chromosome positive (Ph+) leukemia is the BCR/ABL fusion protein. BCR/ABL is characterized by a deregulated and constitutively activated ABL tyrosine kinase (TK) activity.[1] Multiple downstream signaling pathways activated by BCR/ABL including RAS, JAK/STAT, phosphatidylinositol-3-kinase (PI3K) and MYC[1–3] contribute to the transformation potential of BCR/ABL. The expression of BCR/ABL alone is sufficient to induce a leukemic phenotype in mice.[4,5] Cellular transformation and leukemogenesis are strictly dependent on the TK activity of BCR/ABL.[6–9]

Molecular-targeted therapy with the ABL-kinase inhibitor Imatinib Mesylate (Imatinib) induces complete hematological and cytogenetic remissions in the majority of Ph+ leukemia patients.[10] A growing concern is that during advanced disease stages, Imatinib-resistant relapse frequently occurs mainly because of point mutations in the ABL-kinase domain that interfere with the binding affinity of Imatinib.[11,12]

The deregulated activation of the ABL TK is accompanied by phosphorylation-dependent conformational changes.[13] Imatinib selectively binds to and stabilizes the inactive ABL kinase conformation.[14] The key event for the activation of the BCR/ABL kinase is the tetramerization mediated by the N-terminal coiled coil (CC) region of the BCR-portion.[15,16] Accordingly, tetramerization deficient CC-deletion mutants (ΔCC-BCR/ABL) exhibit decreased TK-activity, resulting in the reduction of autophosporylation and the suppression of the transformation potential of BCR/ABL.[15,16] The capacity of ΔCC-BCR/ABL to mediate factor-independence of hematopoietic cell lines is weak[15,17,18] and highly sensitive to Imatinib.[15]

Within the CC, the amino acid (a.a.) residues 5–15 and 28–67 form helices (Helix alpha 1 and alpha 2) separated by a flexible loop. The dimer interface is formed by the direct interaction of Helices-2 of both monomers, while Helix-1 from one monomer swings back and packs against the "outside" of the Helix-2 dimer and interacts with Helix-2 of the other monomer.[19] Helix-2 deletion leads to impaired oligomerization and reduced kinase activity,[20] suggesting a fundamental role of Helix-2 for the biology of BCR/ABL.

Recently, we have shown that a peptide, representing the CC (a.a 1-63), interferes with BCR/ABL tetramerization and counteracts the kinase activity and transformation potential of BCR/ABL accompanied by an increased sensitivity for Imatinib.[15]

The aim of this study was to further develop the CC targeting peptide and to determine how the inhibition of oligomerization interferes with the transformation potential of BCR/ABL and its Imatinib-resistant mutants.

Material and methods

cDNA constructs and retroviral vectors

Helix-1 and Helix-2 encoding sequences harboring both a 5′ BamHI site and a 3′ EcoRI site were generated by PCR on a unmutated $p185^{(BCR/ABL)}$ cDNA as template with the following oligos: Helix-1 (forward primer 5′-GTG GAT CCA CCA TGG TGG ACC CGG TG-3′, reverse primer 5′-CTG AAT TCA GTC CGG GAA CTG CGC CTT CC-3′), Helix-2 (forward primer 5′-AAG GAT CCA CCA TGG AGC TGC GCT CAG TGG G-3′, reverse primer 5′-ATG AAT TCA CCG GTC ATA GCT CTT CTT TTC CTT GGC-3′). PCR products were controlled by sequencing and fused to the GST in pGEX4T3 (Amersham/Pharmacia, Freiburg, Germany) using the BamHI and EcoRI sites. The GST-CC-fusion has been previously described.[15]

Helix-2 and GFP were fused by a "megaprimer" PCR (Helix-2-GFP). Megaprimers were generated using the following oligos: 5′-megaprimer (flanking forward primer 5′-AGA CTG AAG CTT CCA CCA TGG AGC TGC GCT CAG TGG G-3′, reverse primer 5′-ACA GCT CCT CGC CCT TGC TCAC CAT CTC GAG CCG GTC ATA GCT CTT CTT TTC C-3′), 3′megaprimer (forward primer 5′-GGA AAA GAA GAG CTA TGA CCG GCT CGA GAT GGT GAG CAA GGG CGA GGA GC-3′, flanking reverse primer 5′- AAT ACC *AAG CTT* TTA CTT GTA CAG CTC GTC CAT GCC-3′). Megaprimers were purified and used together with the flanking forward and flanking reverse primer in a second PCR.

Grant sponsor: Deutsche José Carreras Leukämie-Stiftung e.V.; Grant number: DJCLS 2001/NAT-1; Grant sponsor: Deutsche Forschungsgemeinschaft; Grant number: DFG 728/3-1; Grant sponsors: the Alfred and Angelika Gutermuth Foundation; AIRC, the "Istituto Pasteur Fondazione Cenci Bolognetti," Università di Roma "La Sapienza".
***Correspondence to:** Labor für Tumorstammzellbiologie, Med. Klinik II/Hämatologie, Klinikum der J.W. Goethe Universität Frankfurt, Theodor Stern Kai 7, 60590 Frankfurt, Germany. Fax: +49-69-6301-6131.
E-mail: ruthardt@em.uni-frankfurt.de
Received 2 October 2007; Accepted after revision 4 January 2008
DOI 10.1002/ijc.23467
Published online 25 March 2008 in Wiley InterScience (www.interscience.wiley.com).

The resulting Helix-2-GFP sequence was directly cloned into the PIDE vector using the Hind III restriction sites (PIDE-Helix-2-GFP) or blunt end into a EcoRV and DraI digested pENTR1A (Invitrogen, Karlsruhe, Germany) for the generation of a Gateway® (Invitrogen) entry vector (pE-Helix-2-GFP).

$p185^{(BCR/ABL)}$ constructs harboring point mutations related to Imatinib-resistance (Y253F, E255K, T315I) were created from unmutated $p185^{(BCR/ABL)}$ cDNA[15] by using the QuikChange® II Site-Directed Mutagenesis Kit (Stratagene; La Jolla, CA) according to the manufacturer's instructions. The following primers were used: $p185^{(BCR/ABL)\text{-}Y253F}$ (forward primer 5′-GGG CGG GGG CCA GTT TGG GGA GGT GTA CGA GGG C-3′) reverse primer 5′-CCT CGT ACA CCT CCC CAA ACT GGC CCC CGC CCA GC-3′), $p185^{(BCR/ABL)\text{-}E255K}$ (forward primer 5′-GGG CCA GTA CGG GAA GGT GTA CGA GGG CGT G-3′, reverse primer 5′-CAC GCC CTC GTA CAC CTT CCC GTA CTG GCC C-3′), $p185^{(BCR/ABL)\text{-}T315I}$ (forward primer 5′-GTT CTA TAT CAT CAT AGA GTT CAT GAC CTA C-3′, reverse primer 5′-GGT CAT GAA CTC TAT GAT GAT ATA GAA CGG-3′). PCR-products were controlled by sequencing and cloned into the EcoRI site of pENTR1A.

The cDNA encoding constitutively active murine c-Kit harboring the D814H mutation[21] inserted into PINCO was kindly provided by Xiaomin Zheng (Memorial Sloan Kettering Cancer Center, NY).

All retroviral expression vectors used in this study were based on the bi-cistronic vector PINCO.[22] The following PINCO variants were created through conventional cloning techniques: PIDE (PINCO lacking GFP), PIDEΔCMV (PINCO lacking the CMV-promotor and GFP) and PAULO (PIDE harboring the functionally inactive "low affinity growth factor receptor" {ΔLNGFR} as a reporter). These vector variants as well as pCDNA3 and pGEX4T3 were converted into Gateway®-destination vectors by the introduction of a Gateway® cassette according to the manufacturer's instructions (Invitrogen). All related inserts were cloned into the Gateway® entry-vector (pENTR1A) for recombination into the destination vectors by using the "LR-clonase" enzyme kit (Invitrogen). PIDEp185-CC-GFP and the pENTR1A encoding CC-GFP (pE-CC-GFP) were described before.[15]

Cell lines, cell culture, imatinib

Ba/F3 cells were maintained in RPMI 1640 medium supplemented with 10% fetal calf serum (FCS) (Invitrogen) containing 10 ng/ml IL-3 (Cell Concepts, Umkirch, Germany). Ecotropic Phoenix cells, 293T, Rat-1 and COS-1 cells were cultured in DMEM supplemented with 10% FCS. Nalm-6, BV-173 and SupB15 cells were provided by the German Collection of Microorganisms and Cell Cultures (DSMZ, Braunschweig, Germany) and maintained in RPMI supplemented with 10% FCS and RPMI supplemented with 15% FCS, respectively. Imatinib was dissolved in 0.1 N HCl and stocked at 10 μM solution at 4°C.

Retroviral infection and transfection

Ecotropic and amphotropic retroviral supernatants (rSN) were obtained as described before.[23,24] For infection of target cells, retronectin® (Takara Bio, Otsu, Japan) was used to enhance infection efficiencies following the manufacturers instructions. 2×10^5 target cell/well were plated. Infection efficiency was measured after 48 hr by determining the percentage of GFP- or ΔNGFR-positive cells by FACS analysis.

Stable transfected Ba/F3 cells were obtained using the Nucleofector® technology according to the manufacturers' instruction (Amaxa Biotechnology, Köln, Germany). Selection with 0.75 μg/ml puromycin was performed for 4 days in the presence of IL-3. Clonal selection of retrovirally infected Ba/F3 cells was performed by limiting dilution. GFP-expressing cells were sorted using the FACSAria cell sorter (BD Biosciences, Heidelberg, Germany).

Proliferation-competition assays

For modified proliferation-competition assays (PCA)[25] Ba/F3 cells were infected with PAULO vectors harboring unmutated and mutant $p185^{(BCR/ABL)}$ or activated $c\text{-}Kit^{D814H}$. IL-3 was removed from the media of infected Ba/F3 cells by washing the cells twice with phosphate buffered saline (PBS). The cells were continuously cultivated in absence of IL-3 and superinfected with GFP, CC-GFP and Helix-2-GFP. Day 4 GFP-expression levels were used to normalize the expression levels of different experiments. Proliferation-competition between single and double infected cell fractions was monitored by FACS analysis of the GFP expression (Fig. 3*a*). Similarly, GFP expression was followed in Nalm-6, SupB15 and BV173 cells infected with GFP, CC-GFP and Helix-2-GFP.

Transformation assays

For soft-agar and focus formation assays Rat-1 fibroblasts were co-transduced with GFP or Helix2-GFP and PAULO vectors harboring unmutated and mutant $p185^{(BCR/ABL)}$. Six-well-plates were filled with 2 ml/well DMEM/10% FCS/0.5% bactoagar (DIFCO Laboratories, Detroit, USA). 5000 Rat-1 cells were plated in 1 ml/well topagar (DMEM/10% FCS/ 0.25% bactoagar). Rat-1 colonies were counted after 15 days incubation at 37°C, 5% CO_2. For focus-formation assays in a 24-well plate format 40,000 double-infected Rat-1 cells were plated per well. After 72 hr Imatinib was added to a final concentration of 0.2–0.6 μM for unmutated $p185^{(BCR/ABL)}$ expressing cells and 1.5–3 μM for cells expressing mutant $p185^{(BCR/ABL)}$. Foci were stained after 15 days using 1% crystal violet (Sigma-Aldrich, Steinheim, Germany).

Western blot

Western blot analyses were performed according to widely established protocols. The following antibodies were used: anti-ABL (α-ABL)(St. Cruz Biotechnology, Santa Cruz, CA), anti-phosphorylated ABL specific for the phosphorylated tyrosine-residues 245 and 412 (α-p-ABL-Tyr-245 and α-p-ABL-Tyr-412)(both Upstate-Biotechnology, Lake Placid, NY). Blocking and antibody incubation were performed in 5% low fat dry milk followed by washing in Tris-buffered saline (TBS)(10 mM Tris-HCl pH 8, 150 mM NaCl) containing 0.1% Tween20 (TBS-T).

Recombinant GST-fusion proteins and "pull-down" assays

The GST, GST-CC, GST-Helix-1 and GST-Helix-2 proteins were produced in *E. coli* BL21 transformed with the respective pGEX4T3 vector upon induction with 0.1 mM isopropyl thiogalactoside (IPTG). Bacterial lysates were prepared in E1A buffer (50 mM HEPES pH 7.8, NaCl 150 mM, EDTA 5 mM, DTT 1 mM, NP40 0.1%), cleared by centrifugation (10 min at 10,000*g*) and incubated for 2 hr at 4°C with equilibrated Glutathione-sepharose beads (Amersham/Pharmacia Biotech, Freiburg, Germany). The beads were washed twice with E1A buffer and bound protein was quantified on a coomassie stained SDS-PAGE gel by comparison to a bovine serum albumin (BSA) standard curve. For "pull-down" experiments, $p185^{(BCR/ABL)}$ expressing Ba/F3 cells were resuspended in E1A lysis buffer (NaCl 150 mM). Cell lysates were treated by sonication and clarified by centrifugation (10 min. at 10,000*g*). One microgram of total protein was incubated with 10 μg immobilized GST or GST-fusion proteins for 1 hr at 4°C. The bound proteins were eluted by boiling in 30 μl 2× SDS-PAGE loading buffer, resolved by SDS-PAGE and visualized by α-ABL antibody.

Coimmunoprecipitation

Lysates of IL-3 independent Ba/F3 cells co-expressing either GFP or Helix-2-GFP together with unmutated or mutant $p185^{(BCR/ABL)}$ were prepared in RIPA-buffer.[26] Lysate volumes corresponding to 500 μg total protein were used for co-immunoprecipitation. After preclearing with 20 μl equilibrated protein-A sepharose slurry (Amersham/Pharmacia Biotech), 3 μL α-GFP antibody (St. Cruz Biotechnology) and 20 μl protein-A sepharose

slurry were used to precipitate GFP from the lysates. Co-precipitated p185$^{(BCR/ABL)}$ proteins were detected by Western blotting using α-ABL antibodies.

Characterization of high molecular weight complexes

The formation of HMW was detected as previously described.[15] Both COS-1 cells expressing p185$^{(BCR/ABL)}$ and GFP or Helix-2-GFP, respectively, and IL-3-independent Ba/F3 cells expressing p185$^{(BCR/ABL)}$ and GFP or Helix-2-GFP were used. Cytosolic extracts were prepared from 1 to 5 × 10^8 cells and fractionated at 4°C by HPLC using a Superose 6 HR 10/30 size exclusion column (Amersham/Pharmacia Biotech). The flow rate was 0.4 ml/min. Fractions of 0.4 ml were pulled, concentrated and analyzed by Western blotting as described above.

Results

The CC helix-2 but not helix-1 interacts with p185$^{(BCR/ABL)}$

We have previously shown that a peptide of the a.a. 1-63 representing the N-terminal BCR coiled coil oligomerization interface (CC) interacts with and inhibits p185$^{(BCR/ABL)}$ kinase activity.[15] The CC domain is composed of two α-helices, Helix-1 and 2 (Fig. 1*a*). Previous data on deletion mutants and crystal structures suggest that Helix-2 mediates the protein-protein interaction by the CC domain.[19,20] To definitively determine the relevant protein-protein interaction interface in the CC domain, we investigated the capacity of peptides encompassing Helix-1 (a.a.1–17) and Helix-2 (a.a. 23–72), respectively, to bind p185$^{(BCR-ABL)}$. Therefore, recombinant GST-Helix-1 and GST-Helix-2 fusion proteins immobilized on glutathione-sepharose beads were used as a bait to precipitate p185$^{(BCR/ABL)}$ from lysates of Ba/F3 cells expressing p185$^{(BCR/ABL)}$. GST alone and the previously described GST-CC,[15] were used as a negative and positive control, respectively. Sepharose-bound protein complexes were separated by SDS-PAGE and analyzed by α-ABL Western blotting. As depicted in Figure 1*b*, only GST-Helix-2 was able to precipitate p185$^{(BCR/ABL)}$ from the cell lysates to the same extent as GST-CC.

These data indicate that Helix-2 represents the oligomerization interface of BCR and thus mediates the interaction between p185$^{(BCR/ABL)}$ monomers.

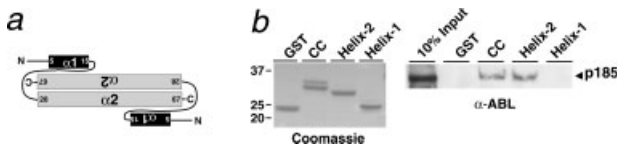

FIGURE 1 – Interaction of coiled-coil subdomains with p185$^{(BCR/ABL)}$. (*a*) Modular organization of the BCR-coiled-coil domain adapted from Zhao *et al*. Helix-1 spans from a.a.5–15, Helix-2 spans from a.a. 28–67.[19] (*b*) Expression of recombinant proteins in *E. coli* and "pull-down" experiment: the coomassie staining (left side) shows the purity and integrity of the indicated constructs expressed in *E. coli* BL21. Lysates from p185$^{(BCR/ABL)}$ expressing Ba/F3 cells were incubated with the indicated GST-fusion constructs immobilized on GST-sepharose beads. The precipitation of interacting p185$^{(BCR/ABL)}$ was detected by Western blotting using an α-ABL antibody.

Co-expression of helix-2 disrupts p185$^{(BCR/ABL)}$ tetramers

The tetramerization of p185$^{(BCR/ABL)}$ is reflected by the formation of intracellular HMW complexes. In fact, the size of complexes formed by a deletion mutant lacking the N-terminal CC domain is markedly reduced as compared to unmutated p185$^{(BCR/ABL)}$.[15]

To investigate whether it is possible to disrupt the p185$^{(BCR/ABL)}$ HMW-complexes by the presence of Helix-2, we co-expressed p185$^{(BCR/ABL)}$ with either GFP or Helix-2-GFP in Cos-1 cells (Fig. 2*a*). Cell lysates were separated by size-exclusion-HPLC. The single HPLC-elution fractions were then subjected to α-ABL Western blot analysis. Upon co-expression with GFP, p185$^{(BCR/ABL)}$ was found in complexes with an apparent MW between 670 and 1,070 kDa (Fig. 2*b*), whereas the presence of Helix-2 led to the detection of p185$^{(BCR/ABL)}$ complexes with apparent MW between 440 and 1,070, with a marked peak at 670 kDa. Endogenous c-ABL complexes displayed an apparent MW of 440–670 kDa, which was not influenced by the presence of GFP or Helix-2-GFP (Fig. 2*b*).

Taken together, these data indicate that binding to Helix-2 interferes with the oligomerization of p185$^{(BCR/ABL)}$ as revealed by the reduction of the size of its HMW-complexes.

Helix-2 reduces the autophosphorylation of p185$^{(BCR/ABL)}$ and increases the sensitivity of p185$^{(BCR/ABL)}$ towards Imatinib

The fact that Helix-2 disrupted the p185$^{(BCR/ABL)}$ HMW-complexes prompted us to investigate whether the Helix-2 peptides have inhibitory effects on p185$^{(BCR/ABL)}$ expressing cells as compared to the known effects of the CC-peptides.[15]

Hence, we investigated the autophosphorylation of p185$^{(BCR/ABL)}$ in the presence of CC-GFP and Helix-2-GFP. Therefore, we analyzed Ba/F3 cells stably co-expressing p185$^{(BCR/ABL)}$ in the presence of either GFP, CC-GFP or Helix-2-GFP by Western blotting with an α-phospho-ABL antibody (α-P-ABL-Y245) and an

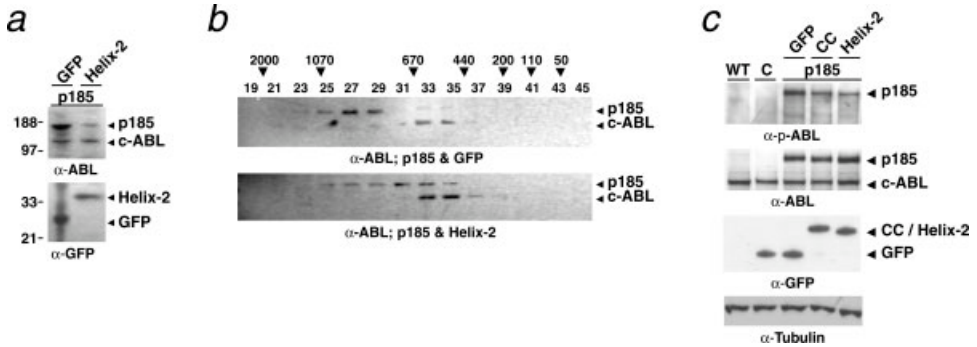

FIGURE 2 – Disruption of p185$^{(BCR/ABL)}$ high molecular weight complexes and reduction of p185$^{(BCR/ABL)}$ autophosphorylation by helix-2. (*a*) Western blot analysis of cytoplasmic extracts of transfected Cos-1 cells. The cells were cotransfected as indicated either with GFP and p185$^{(BCR/ABL)}$ or helix-2-GFP and p185$^{(BCR/ABL)}$. The expression of the transgenes was determined by α-GFP and α-ABL antibodies. (*b*) The cytoplasmic extracts of cotransfected Cos-1 cells were fractionated by size-exclusion HPLC. p185$^{(BCR/ABL)}$ was detected in the fractions by an α-ABL Western blot. The blots show the presence of p185$^{(BCR/ABL)}$ in fractions corresponding to the molecular weight (MW) indicated at the top. (*c*) Ba/F3 cells stably expressing the indicated transgenes were lysed and phosphorylation at ABL-tyrosine residue 245 was analyzed by Western blot using an α-ABL(Tyr-245) specific antibody. The membrane was repeatedly stripped and probed with the indicated antibodies. One representative experiment out of 3 is given.

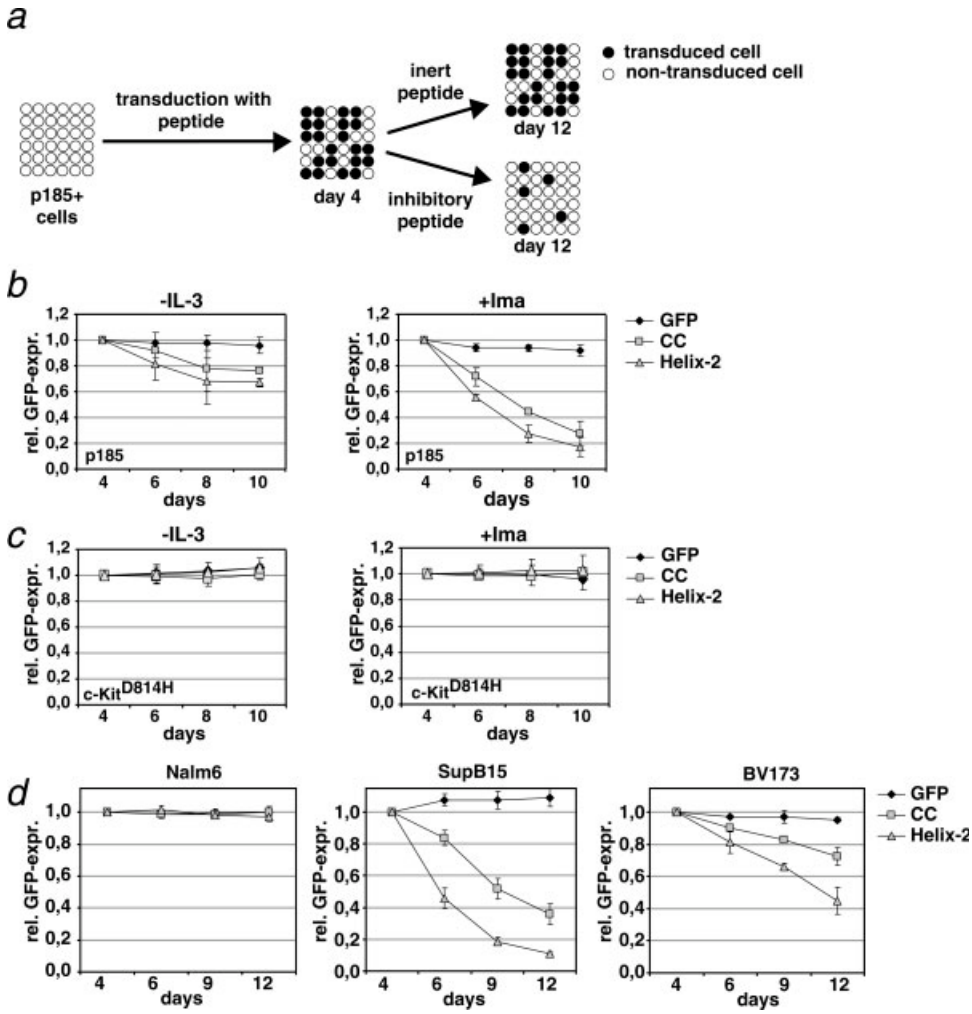

FIGURE 3 – Growth inhibition of p185$^{(BCR/ABL)}$ expressing Ba/F3 cells and Philadelphia chromosome positive human cell lines. (*a*) Schematic representation of a proliferation-competition assay. Factor independent cells (*e.g.*, p185$^{(BCR/ABL)}$ expressing Ba/F3 cells) are retrovirally infected with inert control peptides (GFP) or inhibitory peptide-GFP fusions (CC-GFP or Helix-2-GFP). In the case of the inert GFP control the percentage of GFP-positive cells remains constant from day 4 to day 12. In contrast, the expression of inhibitory peptides results in an outgrowth of peptide expressing cells revealed by a progressive loss of Helix-2-GFP expression. (*b* and *c*) For proliferation-competition experiments p185$^{(BCR/ABL)}$ or c-Kit^{D814H} transduced Ba/F3 cells adapted to factor independence were infected with GFP, CC-GFP or Helix-2-GFP expressing retroviruses and replated 4 days after infection in the presence or absence of subapoptotic Imatinib (Ima) concentrations (0.4 μM). The proportion of the GFP-positive cell fraction was followed by flow cytometry for 10 days and normalized to the GFP expression at day 4. Graphs show mean values of three independent experiments ±SD. (*d*) Proliferation competition assays were performed with the human B-cell precursor cell lines Nalm-6 (Ph-), SupB15 (Ph+) and BV173 (Ph+). These cells were infected with GFP, CC-GFP or Helix-2-GFP expressing retroviruses. The proportion of GFP-positive cell fraction was followed by FACS for 10 days and normalized to the GFP expression at day 4. Graphs show mean values of 3 independent experiments ±SD.

α-ABL antibody. As depicted in Figure 2*c* the presence of Helix-2 reduced the level of p185$^{(BCR/ABL)}$ autophosphorylation to the same extent as CC.

To assess whether the inhibited autophosphorylation of p185$^{(BCR/ABL)}$ by Helix-2 interferes with the survival of cells transformed by p185$^{(BCR/ABL)}$, we performed proliferation competition experiments on p185$^{(BCR/ABL)}$ expressing Ba/F3 cells. The principle of the assay is depicted in Figure 3*a*: Ba/F3 cells transduced with the retroviral vector PAULOp185 were selected by IL-3 withdrawal for 7 days, resulting in bulk populations that uniformly coexpress p185$^{(BCR/ABL)}$ and ΔLNGFR. Thereafter, these cells were transduced with retroviral vectors harboring GFP, CC-GFP or Helix-2-GFP. The resulting double infected cell populations were then exposed to a sub-apoptotic Imatinib concentration (0.4 μM) for p185$^{(BCR/ABL)}$ expressing Ba/F3 cells (data not shown).[15] The effect of the transduced peptides was assessed by the detection of GFP positive cells for 1 week by FACS. The GFP-expression on day 4 was taken as a reference for normalization. As shown in Figure 3*b*, the expression of GFP did not alter the proliferation of p185$^{(BCR/ABL)}$ expressing Ba/F3 cells as revealed by the constant percentage of GFP positive cells. In contrast, CC and Helix-2 inhibited the growth of p185$^{(BCR/ABL)}$ expressing Ba/F3 cells as shown by the fact that the percentage of CC-GFP or Helix-2-GFP expressing cells decreased over time with comparable kinetics (Fig. 3*b*). The addition of Imatinib accelerated the decrease of CC-GFP- or Helix-2-GFP expressing cells, but had no influence on GFP controls (Fig. 3*b*). To exclude effects of the peptides not related to their binding to p185$^{(BCR/ABL)}$ and to prove the specificity of their effects, we performed the same experiments with Ba/F3 cells expressing a constitutively activated murine c-Kit, the mutant c-Kit^{D814H}.[21] The c-Kit^{D814H} mediates factor independence to the same extent as p185$^{(BCR/ABL)}$, which was also reverted by 2 μM Imatinib (Zheng et al., submitted). The co-expression of Helix-2- or CC-GFP-fusion peptides did not

inhibit the growth of c-Kit^{D814H}-expressing IL-3 independent cells either in the absence or presence of Imatinib (Fig. 3*c*).

Taken together, these results show that the Helix-2 peptide inhibits the p185$^{(BCR/ABL)}$ kinase activity to the same extent as the previously described CC-peptide inducing both growth suppression of p185$^{(BCR/ABL)}$-dependent cells and an increased sensitivity for Imatinib.

Helix-2 specifically inhibits Ph+ human cell lines

To confirm the effects of Helix-2 on human Ph+ patient derived cells, we performed the proliferation competition experiments on human Ph+ cell lines derived from ALL or CML patients. We used SupB15 (Ph+ ALL) expressing p185$^{(BCR/ABL)}$, BV-173 (lymphatic CML blast crisis) expressing p210$^{(BCR/ABL)}$ and as a BCR/ABL-negative control the Ph- Nalm-6 cells, because all these cells exhibited a nearly identical pre-B lymphatic differentiation level.[27] These cells were retrovirally infected with GFP, CC-GFP or Helix-2-GFP. The GFP-expression was determined for 12 days after infection with the day 4 expression as a reference. In contrast to the Ph- Nalm-6 cells, which exhibited a constant GFP, CC-GFP or Helix-2 expression, in the Ph+ SupB15 and BV173 cells the percentages of CC-GFP and Helix-2-GFP positive cells decreased over time, whereas the GFP expression was constant. The kinetics of the outgrowth of Helix-2-GFP positive cells was accelerated with respect to that of CC-GFP positive cells (Fig. 3*d*).

To obtain 100% infected human cells, we sorted CC-GFP and Helix-2-GFP expressing cells. While Nalm-6 cells transduced with GFP, Helix-2-GFP or CC-GFP rapidly proliferated after sorting, BV173 and SupB15 cells only infected with GFP but not with CC-GFP or Helix-2-GFP grew up after sorting. The fact that we were unable to generate SupB15 and BV173 cells stably expressing CC-GFP or Helix-2-GFP is attributed to inhibitory effects of the peptides BCR/ABL (data not shown).

Taken together these data show that patient derived Ph+ cell lines are specifically inhibited by peptides targeting the N-terminal oligomerization interface of BCR/ABL and that Helix-2 seems to be more effective than CC in the inhibition of BCR/ABL.

Helix-2 interacts with mutant p185$^{(BCR/ABL)}$ and disrupts the HMW-complexes of imatinib-resistant p185$^{(BCR/ABL)}$ point mutants

The acquisition of point mutations, which decrease the affinity of competitive TK-inhibitors such as Imatinib, Dasatinib or Nilotinib to the ATP-binding site of BCR/ABL, is the best studied mechanism for resistance against kinase inhibitors.[28–30] To assess whether the inhibition of tetramerization by Helix-2-peptides is able to inhibit Imatinib-resistant p185$^{(BCR/ABL)}$ we evaluated the effects of Helix-2 on 3 clinically relevant mutations responsible for Imatinib-resistance — two P-loop mutations Y253H and E255K, and the "gatekeeper" T315I mutation.

As the interaction of Helix-2 with mutant p185$^{(BCR/ABL)}$ and its capacity to disrupt the p185$^{(BCR/ABL)}$ tetramerization are required for its inhibitory effects, we first investigated whether Helix-2 interacts with mutant p185$^{(BCR/ABL)}$ and disrupts the HMW-complexes of mutant p185$^{(BCR/ABL)}$. Therefore, lysates of IL-3 independent Ba/F3 cells co-expressing either unmutated p185$^{(BCR/ABL)}$ or its mutants together with GFP or Helix2-GFP were used for co-immunoprecipitation as well as for size-exclusion HPLC as described above.

The co-immunoprecipitation by an α-GFP antibody and subsequent α-ABL Western blotting showed that the p185$^{(BCR/ABL)}$ mutants bind to Helix-2 like unmutated p185$^{(BCR/ABL)}$ (Fig. 4*a*). Noteworthy, in contrast to GFP, the presence of Helix-2 in these factor-independent cell populations seemed to select cells with high expression levels of p185$^{(BCR/ABL)}$, p185$^{(BCR/ABL-Y253F)}$ and p185$^{(BCR/ABL-E255K)}$, but not of p185$^{(BCR/ABL-T315I)}$ (Fig. 4*a*).

The analysis of p185$^{(BCR/ABL)}$ HMW-complex formation by size-exclusion-HPLC revealed no differences between unmutated p185$^{(BCR/ABL)}$, and the mutants p185$^{(BCR/ABL-Y253F)}$ and p185$^{(BCR/ABL-E255K)}$, in the presence of GFP. In fact, all these p185$^{(BCR/ABL)}$ forms were found in HMW fractions corresponding to an apparent MW between 670 and 1070 kDa, peak fractions corresponding to about 800–900 kDa (fractions no. 27–29) (Fig. 4*b*). In contrast, the pattern of HMW-complexes formed by

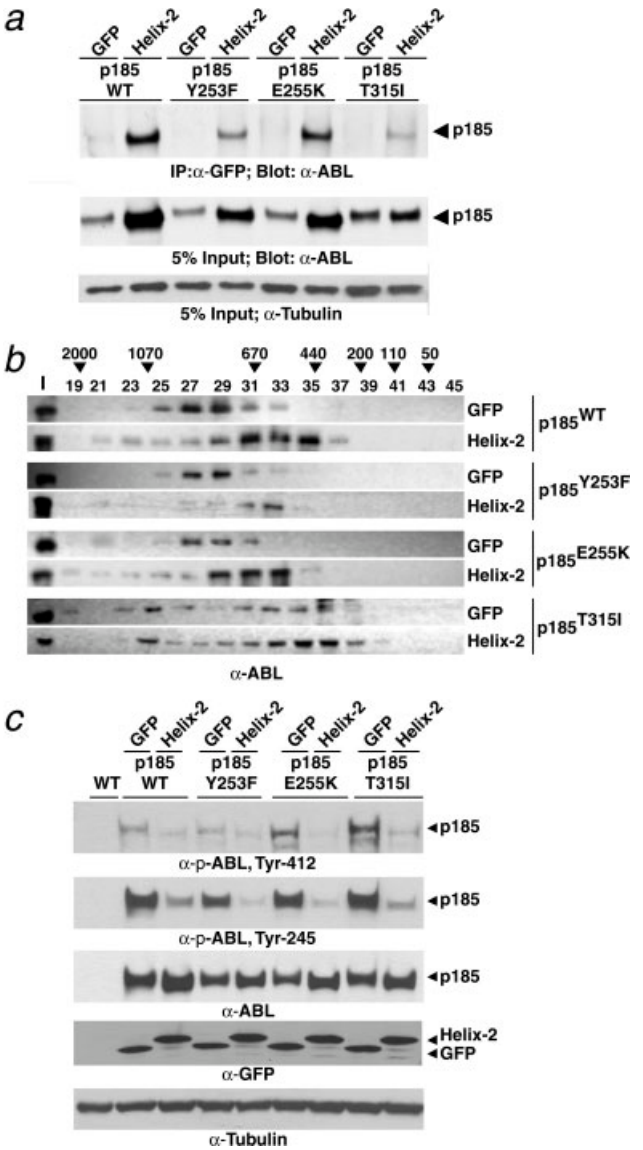

FIGURE 4 – Helix-2 Interacts with mutant p185$^{(BCR/ABL)}$, disrupts HMW-complexes and inhibits autophosphorylation of unmutated and mutant p185$^{(BCR/ABL)}$. (*a*) A GFP specific antibody was used to coprecipitate unmutated or mutant p185$^{(BCR/ABL)}$ from lysates of IL-3 independent Ba/F3 cells coexpressing unmutated or mutant p185$^{(BCR/ABL)}$ and either GFP or Helix-2-GFP. Coprecipitated p185$^{(BCR/ABL)}$ was detected by Western blot with an α-ABL antibody. Five percentage of the protein amount used is given as input, an α-Tubulin antibody was used to show equal loading. (*b*) Cytoplasmic extracts of IL-3 independent Ba/F3 cells coexpressing the indicated p185$^{(BCR/ABL)}$ constructs and either GFP or Helix-2-GFP were fractionated by size-exclusion HPLC. p185$^{(BCR/ABL)}$ was detected in the fractions by an α-ABL Western blot. (*c*) Autophosphorylation of Mutant p185$^{(BCR/ABL)}$ in presence of Helix-2 peptides. Lysates of GFP or Helix-2-GFP Ba/F3 cell clones infected with unmutated or mutant p185$^{(BCR/ABL)}$ were blotted and probed with an α-ABL(Tyr-245) specific antibody, stripped and reprobed with an α-ABL(Tyr-412) specific antibody. The membrane was repeatedly stripped and probed with the indicated antibodies. One representative experiment out of 3 is given.

$p185^{(BCR/ABL-T315I)}$ is different as compared to unmutated $p185^{(BCR/ABL)}$. $p185^{(BCR/ABL-T315I)}$ predominantly forms complexes of about 1070 kDa (fraction no. 25), while it is hardly detectable in fractions corresponding to 800–900 kDa. In addition, $p185^{(BCR/ABL-T315I)}$ forms complexes of a MW between 670 and 400 kDa, which in the case unmutated $p185^{(BCR/ABL)}$ form only very thin bands. In the presence of Helix-2-GFP we observed a similar size reduction of the HMW-complexes of unmutated $p185^{(BCR/ABL)}$, $p185^{(BCR/ABL-Y253F)}$ and $p185^{(BCR/ABL-E255K)}$ as observed before in transfected Cos-1 cells (Fig. 2*b*). Similarly, Helix-2 influenced the HMW-complex pattern of $p185^{(BCR/ABL-T315I)}$. Helix-2 led to the elution of $p185^{(BCR/ABL-T315I)}$ in fractions corresponding to lower MWs reaching about 200 kDa which are absent in presence of GFP. In contrast, the predominant 1070 kDa fraction (no. 25) formed by the mutant T315I was not influenced by Helix-2 (Fig. 4*b*).

In summary, these data suggest that Helix-2 interacts with $p185^{(BCR/ABL)}$, notwithstanding the presence of point mutations related to the resistance against kinase inhibitors. Contrary to this, the presence of T315I mutations seems to interfere with the capacity of Helix-2 to disrupt HMW-complexes of $p185^{(BCR/ABL)}$.

Helix-2 reduces the autophosphorylation of imatinib-resistant $p185^{(BCR/ABL)}$ mutants

As shown earlier, Helix-2 peptides reduce the autophosphorylation of unmutated $p185^{(BCR/ABL)}$ (Fig. 2*c*). To evaluate the inhibitory effects of Helix-2 peptides on the tyrosine-kinase activity of mutant $p185^{(BCR/ABL)}$, we studied the influence of Helix-2-GFP on the phosphorylation status of $p185^{(BCR/ABL)}$ and its mutants at two phospho-tyrosine residues critical for ABL-activation (Y245 and Y412).[31] Therefore, lysates of Ba/F3 cells co-expressing either unmutated $p185^{(BCR/ABL)}$ or its mutants together with GFP or Helix2-GFP were separated by SDS-PAGE, blotted and probed with phospho-c-ABL specific antibodies. As depicted in Figure 4*c*, the expression of Helix-2 prevented autophosphorylation of $p185^{(BCR/ABL)}$, as well as of its mutants at both phospho-tyrosine residues.

These results provide evidence that Helix-2 inhibits the autophosphorylation of $p185^{(BCR/ABL)}$ independently of its mutation status.

Helix-2 reduces the transforming activity of unmutated and mutant $p185^{(BCR/ABL)}$

We have shown before that the BCC-GFP peptides inhibit the transformation potential of BCR/ABL, as revealed by the inhibition of the anchorage independent growth of $p185^{(BCR/ABL)}$-expressing Rat-1 fibroblasts.[15] To investigate whether Helix-2 peptides exhibit similar inhibitory effects on the transformation potential of mutant $p185^{(BCR/ABL)}$ we co-expressed GFP or Helix-2-GFP and unmutated or mutant $p185^{(BCR/ABL)}$ in Rat-1 cells. The transduction efficiency was assessed by the detection of GFP and ΔLNGFR, respectively. For each construct triplicates of 5,000 double infected Rat-1 cells were plated in soft agar and the colonies were counted after 15 days. As shown in Figure 5A Helix-2 inhibited the colony formation of Rat-1 cells that express either unmutated or mutant $p185^{(BCR/ABL)}$. To assess whether Helix-2 restores the contact inhibition of Rat-1 fibroblasts expressing unmutated or mutant $p185^{(BCR/ABL)}$ we performed focus-formation assays with these double-infected Rat-1 bulks in the presence and absence of Imatinib. At day 15, foci were stained with crystal violet. The expression of Helix-2 restored the contact inhibition of unmutated and less pronounced that of mutant $p185^{(BCR/ABL)}$. With the exception of the mutant T315I, the addition of Imatinib to the growth medium enhanced the restoration of the contact inhibition (Fig. 5*b*).

These data indicate that the disruption of tetramer formation inhibits the transforming capacity of Imatinib-resistant $p185^{(BCR/ABL)}$ mutants and increases the sensitivity towards Imatinib except for the mutant T315I.

Helix-2 inhibits the factor independence and overcomes Imatinib-resistance of hematopoietic cells expressing mutant $p185^{(BCR/ABL)}$ with exception of T315I

To assess whether the disruption of $p185^{(BCR/ABL)}$ HMW-complexes by Helix-2-peptides is able to overcome $p185^{(BCR/ABL)}$-mediated factor independence of hematopoietic cells and the Imatinib-resistance conferred by point mutations, we performed PCAs as described earlier. Transduced IL-3 independent Ba/F3 bulk populations expressing either ΔLNGFR and unmutated $p185^{(BCR/ABL)}$ or ΔLNGFR and $p185^{(BCR/ABL)}$ mutants Y253H, E255K and T315I were superinfected with GFP or Helix-2-GFP. GFP and Helix-2-GFP expression levels were followed for 8 days and expression at day 4 was taken as a reference. Half of the cells were exposed to sub-apoptotic Imatinib concentrations (0.4 μM for unmutated $p185^{(BCR/ABL)}$, 3 μM for mutant $p185^{(BCR/ABL)}$). As shown in Figure 6*a*, the growth of cells expressing unmutated $p185^{(BCR/ABL)}$, $p185^{(BCR/ABL-Y253F)}$ or $p185^{(BCR/ABL-E255K)}$, but not $p185^{(BCR/ABL-T315I)}$ was inhibited by Helix-2-GFP, whereas no effect of GFP was seen. This effect was enhanced by Imatinib with the exception of $p185^{(BCR/ABL-T315I)}$ (Fig. 6*a*). The unresponsiveness of $p185^{(BCR/ABL-T315I)}$ towards Helix-2 apparently contradicts our soft agar data with Rat-1 fibroblasts. To exclude cell line specific effects we extended the experiments on the Il-3 dependent murine myeloid cell line 32D with identical results (Fig. 6*b*).

In summary, these results demonstrated that Helix-2 is able to inhibit the proliferation of Ba/F3 and 32D cells expressing $p185^{(BCR/ABL-E255K)}$ and $p185^{(BCR/ABL-Y253F)}$, but not $p185^{(BCR/ABL-T315I)}$. Except for $p185^{(BCR/ABL-T315I)}$ the co-expression of Helix-2 increases the sensitivity of mutant $p185^{(BCR/ABL)}$ towards Imatinib.

Discussion

The tetramerization and the formation of HMW are crucial for the leukemogenic potential of BCR/ABL, and its inhibition increases the sensitivity for the kinase inhibitor Imatinib.[15–18] The aim of the present study was to further develop the disruption of tetramerization as a therapeutic approach by reducing the size of the inhibiting peptide and exploring its effectiveness on $p185^{(BCR/ABL)}$ mutants related to the resistance against kinase inhibitors such as Imatinib.

Here, we show that the relevant interaction interface in the N-terminal BCR coiled coil region is the 39 a.a. sequence representing the Helix-2. Helix-2 binds to $p185^{(BCR/ABL)}$ to the same extent as the entire CC-domain leading to the disruption of the HMW-complexes of $p185^{(BCR/ABL)}$. This allowed us to explore the effectiveness of the inhibition of the tetramerization using a small peptide which might be utilized in future for the treatment of Ph+ leukemia, or might represent a lead structure for the development of small molecules targeting the tetramerization of BCR/ABL.

The therapeutic relevance of such an approach is given by the fact that the Helix-2 not only inhibited the function of $p185^{(BCR/ABL)}$ in an artificial cell model such as the Ba/F3 and 32D cells retrovirally transduced and selected by IL-3 withdrawal, but also in the patient derived lymphatic Ph+ cell lines, SupB15 and BV173. Regarding the growth inhibition of Ba/F3 cells, the inhibitory effect of Helix-2 was similar to that of the CC-peptide, whereas in BV173 and SupB15 cells the inhibitory effect of Helix-2 was stronger than that of the CC-peptide. Regarding the decrease of $p185^{(BCR/ABL)}$ autophosphorylation, Helix-2 exhibited a similar inhibitory potential than the peptide representing the entire CC-domain.

We assumed that the inhibition of tetramerization by Helix-2 peptides should inhibit the kinase activity and transforming capacity of BCR/ABL irrespective of the presence of point-mutations in the tyrosine kinase domain that confer Imatinib resistance. Consistent with this hypothesis we found that Helix-2 reduces the autophosphorylation of unmutated and mutant BCR/ABL to the same extend. Furthermore, Helix-2 inhibits the anchorage independent growth and restores the contact inhibition of Rat-1

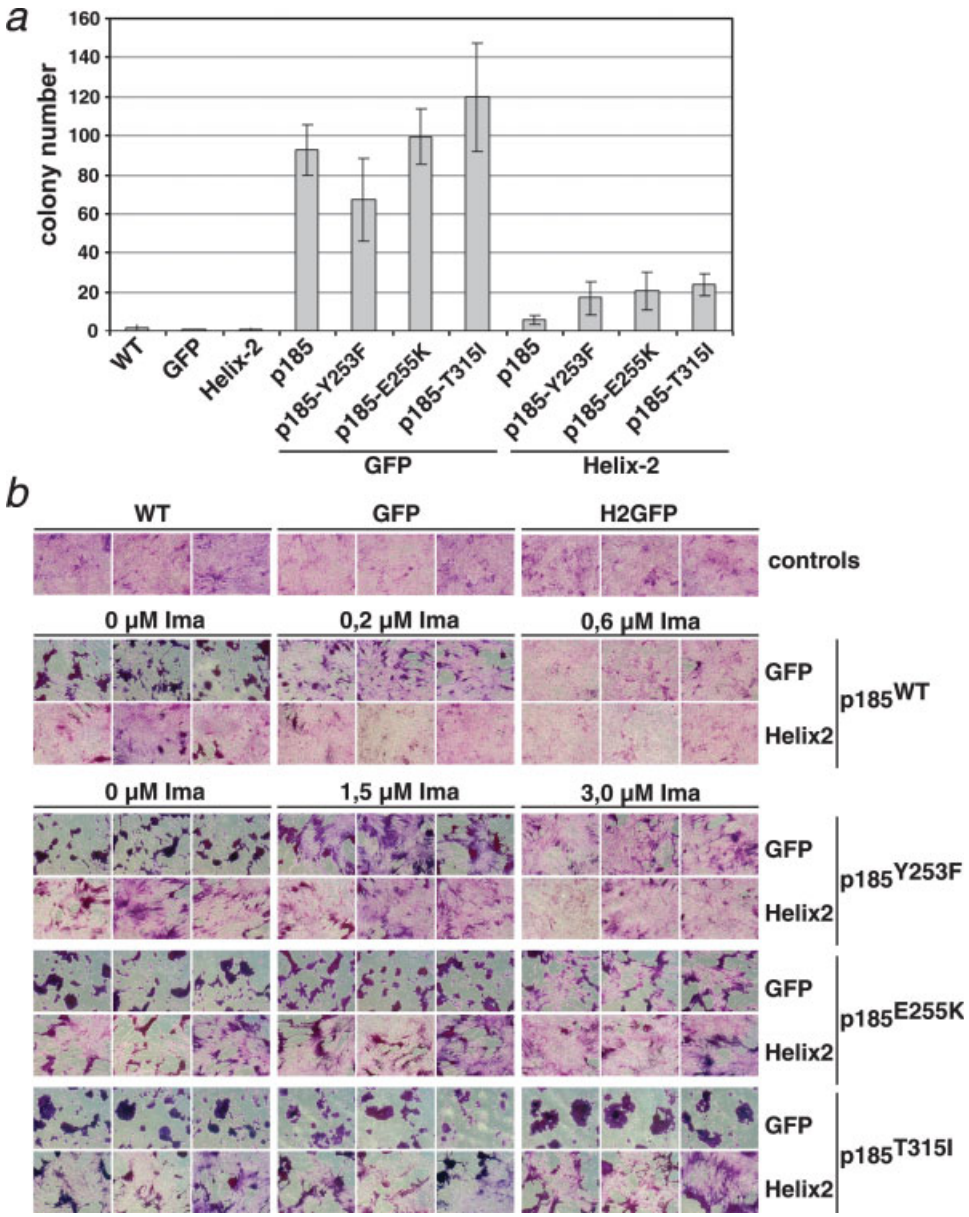

FIGURE 5 – Fibroblast transformation assays. Rat-1 cells were retrovirally transduced with GFP or Helix-2-GFP and overinfected with retroviruses encoding unmutated or mutant $p185^{(BCR/ABL)}$ as indicated. (*a*) 5,000 double infected Rat-1 cells/well were plated in soft-agar in 6-well-plates as described in the material and methods section. After 15 days incubation at 5% CO_2 and 37°C the colonies were counted. Means of triplicates of 2 representative experiments are given ±SD. (*b*) Triplicates of 40,000 double infected Rat-1 cells/well were plated in 24-well-plates. Seventy-two hours later cells reached confluency and were subsequently incubated for additional 12 days in absence or presence of the indicated concentrations of Imatinib. Thereafter the adherent cells were washed twice with PBS, dried and stained with 1% crystal violet. One represenative experiment of 3 is given (×40 magnification).

fibroblasts transformed by unmutated BCR/ABL and partially restores the contact inhibition of mutant BCR/ABL. However, when we analyzed the inhibitory effects of Helix-2 on the factor independent proliferation of hematopoietic cells expressing $p185^{(BCR/ABL)}$ harboring these mutations we revealed unexpected differences in the response of mutant BCR/ABL. Consistent with the inhibitory effects of Helix-2 on BCR/ABL-transformed fibroblasts we found that Helix-2 inhibits unmutated $p185^{(BCR/ABL)}$, $p185^{(BCR/ABL\text{-}E255K)}$ and $p185^{(BCR/ABL\text{-}Y253F)}$ expressing Ba/F3 and 32D cells. In contrast, $p185^{(BCR/ABL\text{-}T315I)}$ expressing hematopoietic cells did not respond to Helix-2. These data indicate that the point mutation T315I induces changes in the biological activity of BCR/ABL which alter the response towards Helix-2. This point mutation seemingly enables $p185^{(BCR/ABL)}$ to mediate factor independence independently of its autophosphorylation. The observation that the unresponsiveness of T315I towards Helix-2 peptides manifests in hematopoietic cells but not in fibroblasts is in accordance to our previously published data: several artificial ABL-chimeras between ABL and the isolated oligomerization domains derived from BCR, TEL, PLZF or PML lead to oligomerization of ABL and confer factor independence but are unable to satisfy classical criteria of oncogenic transformation.[15] The same is true for CC-deletion mutants of BCR/ABL.[15] Furthermore, these data are in accordance to a recently published study showing that $p210^{(BCR\text{-}ABL)}$ mutated at position T315I exhibits an increased transformation capacity of primary bone marrow cells despite a reduced kinase activity.[32] Our HPLC studies revealed specific features of the T315I mutation which might explain the resistance

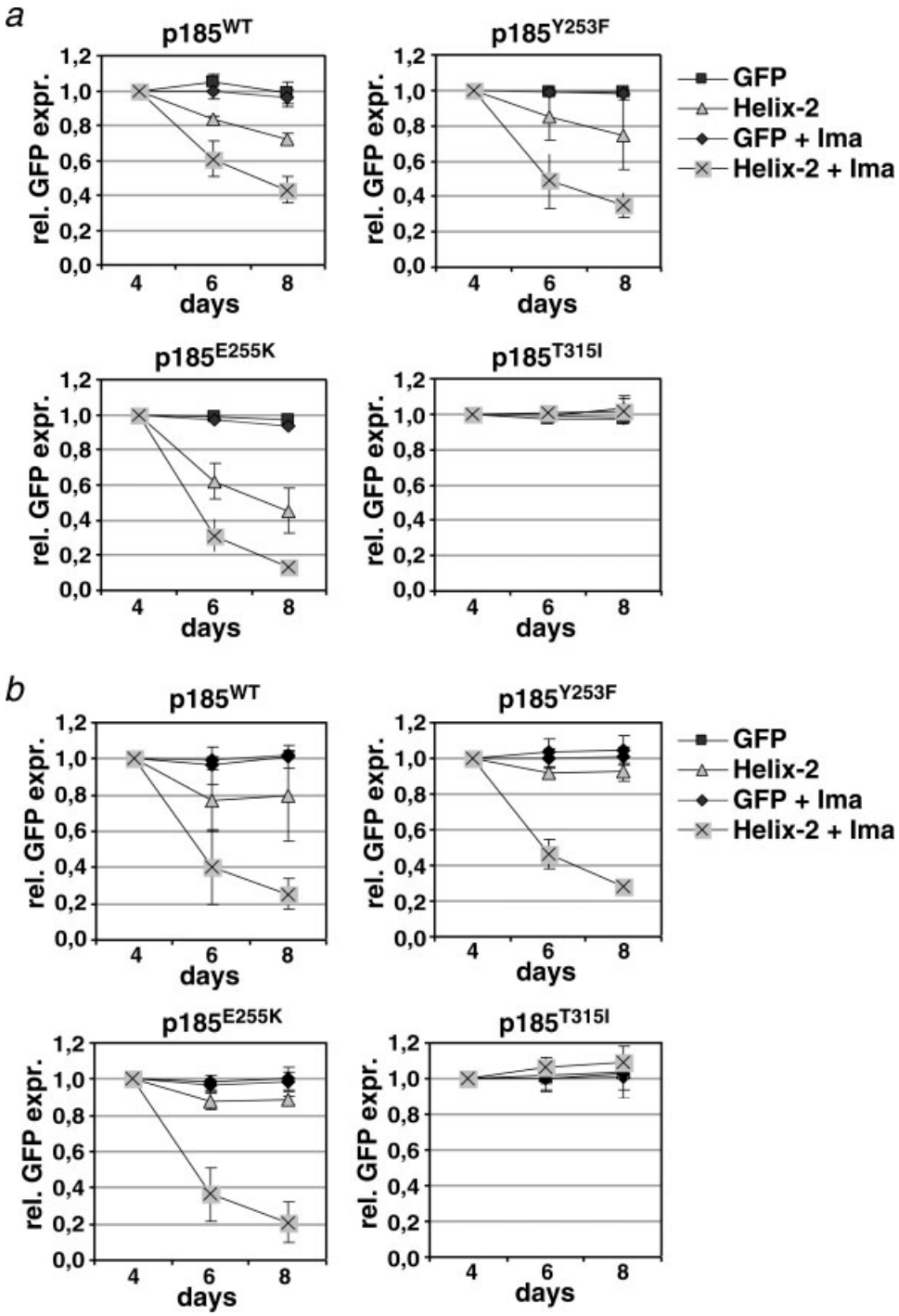

FIGURE 6 – Effect of Helix-2 on BCR/ABL mutants resistant to Imatinib. For proliferation competition experiment WT or mutant $p185^{(BCR/ABL)}$ transduced Ba/F3 cells (*a*) or 32D cells (*b*) adapted to factor independence were infected with GFP or Helix-2-GFP. The cells were replated 4 days after infection in the presence or absence of subapoptotic Imatinib (Ima) concentrations (0.4 μM for WT and 3 μM for mutant $p185^{(BCR/ABL)}$). The proportion of the GFP-positive cell fraction was followed by FACS for 10 days and normalized to the GFP expression at day 4. Graphs show mean values of 3 independent experiments ±SD.

towards Helix-2 peptides: $p185^{(BCR/ABL\text{-}T315I)}$ exhibits a different HMW pattern as compared to unmutated $p185^{(BCR/ABL)}$ and the other mutants. The HMW pattern of $p185^{(BCR/ABL\text{-}T315I)}$ was characterized by two different peaks: (*i*) one of about 1,070 kDa, less pronounced in unmutated $p185^{(BCR/ABL)}$ and absent in the p-loop mutants, which did not respond to the Helix-2; (*ii*) and another peak at lower MW which is not present in unmutated $p185^{(BCR/ABL)}$, was shifted towards even lower MW in the presence of Helix-2 peptides. This $p185^{(BCR/ABL\text{-}T315I)}$-specific HMW-complex pattern might be due to the differences in the stability or the composition of the HMW-complexes. Although we observed HMW-complexes of 1,070 kDa (fraction no. 25) in unmutated $p185^{(BCR/ABL)}$ this fraction was not a peak fraction but the upper limit of the unmutated HMW-pattern. The predominant elution of the $p185^{(BCR/ABL\text{-}T315I)}$ complexes at 1,070 kDa indicates that these complexes exhibit a higher stability as

compared to those formed by unmutated $p185^{(BCR/ABL)}$, which are distributed over a wider MW-range. Furthermore, the $p185^{(BCR/ABL\text{-}T315I)}$ complexes at 1,070 kDa are not disrupted by Helix-2 which also indicates a higher stability. Another reason for the modified HMW-complex pattern of $p185^{(BCR/ABL\text{-}T315I)}$ might also be an aberrant recruitment of unknown binding partners that do not interact with unmutated $p185^{(BCR/ABL)}$. In contrast the HMW-complexes of $p185^{(BCR/ABL\text{-}T315I)}$ of lower MW responded at least partially to Helix-2 peptides. This is in accordance to our co-immunoprecipitation experiments that revealed that Helix-2 binds to $p185^{(BCR/ABL\text{-}T315I)}$. Therefore we can exclude a lack of interaction between Helix-2 and $p185^{(BCR/ABL\text{-}T315I)}$ as a reason for resistance against the peptide. In summary our data indicate that $p185^{(BCR/ABL\text{-}T315I)}$ forms a subset of complexes unresponsive towards Helix-2 that provides a sufficient survival signal.

Regarding the response of mutated BCR/ABL towards Imatinib in presence of Helix-2, we found that Helix-2 expression overcomes the Imatinib-resistance of $p185^{(BCR/ABL\text{-}Y253F)}$ and $p185^{(BCR/ABL\text{-}E255K)}$ but not of $p185^{(BCR/ABL\text{-}T315I)}$. The fundamental difference between T315I and Y253F or E255K might be due to the gatekeeper function of T315. It is widely accepted that Imatinib binds to the inactive ABL-kinase conformation[14] and thus one can hypothesize that the inhibition of the BCR/ABL TK-activity caused by the interaction with Helix-2 is related to conformational changes in the ABL-kinase domain that increase the affinity towards Imatinib of mutations that do not confer complete resistance such as the p-loop mutations.

Here we show for the first time that $p185^{(BCR/ABL)}$ harboring mutations related to Imatinib-resistance are responsive to the inhibition of the tetramerization by Helix-2 in classical transformation assays. This is of particular clinical significance, because it establishes the targeting of the tetramerization interface of BCR/ABL as a new therapeutic approach, which could contribute together with clinical relevant ABL-kinase inhibitors to an improved molecular targeting of BCR/ABL.

References

1. Faderl S, Talpaz M, Estrov Z, O'Brien S, Kurzrock R, Kantarjian HM. The biology of chronic myeloid leukemia. N Engl J Med 1999;341:164–72.
2. Sattler M, Salgia R, Okuda K, Uemura N, Durstin MA, Pisick E, Xu G, Li JL, Prasad KV, Griffin JD. The proto-oncogene product p120CBL and the adaptor proteins CRKL and c-CRK link c-ABL, p190BCR/ABL and p210BCR/ABL to the phosphatidylinositol-3′ kinase pathway. Oncogene 1996;12:839–46.
3. Deininger MW, Goldman JM, Melo JV. The molecular biology of chronic myeloid leukemia. Blood 2000;96:3343–56.
4. Kelliher MA, McLaughlin J, Witte ON, Rosenberg N. Induction of a chronic myelogenous leukemia-like syndrome in mice with v-abl and BCR/ABL. Proc Natl Acad Sci USA 1990;87:6649–53.
5. Huettner CS, Zhang P, Van Etten RA, Tenen DG. Reversibility of acute B-cell leukaemia induced by BCR-ABL1. Nat Genet 2000;24:57–60.
6. Lugo TG, Pendergast AM, Muller AJ, Witte ON. Tyrosine kinase activity and transformation potency of bcr-abl oncogene products. Science 1990;247:1079–82.
7. Deininger MW, Goldman JM, Lydon N, Melo JV. The tyrosine kinase inhibitor CGP57148B selectively inhibits the growth of BCR-ABL-positive cells. Blood 1997;90:3691–8.
8. Druker BJ, Tamura S, Buchdunger E, Ohno S, Segal GM, Fanning S, Zimmermann J, Lydon NB. Effects of a selective inhibitor of the Abl tyrosine kinase on the growth of Bcr-Abl positive cells. Nat Med 1996;2:561–6.
9. Weisberg E, Griffin JD. Mechanism of resistance to the ABL tyrosine kinase inhibitor STI571 in BCR/ABL-transformed hematopoietic cell lines. Blood 2000;95:3498–505.
10. O'Dwyer ME, Mauro MJ, Druker BJ. STI571 as a targeted therapy for CML. Cancer Invest 2003;21:429–38.
11. Cowan-Jacob SW, Guez V, Fendrich G, Griffin JD, Fabbro D, Furet P, Liebetanz J, Mestan J, Manley PW. Imatinib (STI571) resistance in chronic myelogenous leukemia: molecular basis of the underlying mechanisms and potential strategies for treatment. Mini Rev Med Chem 2004;4:285–99.
12. Deininger M. Resistance to Imatinib: mechanisms and management. J Natl Compr Canc Netw 2005;3:757–68.
13. Van Etten RA. c-Abl regulation: a tail of two lipids. Curr Biol 2003;13:R608–R610.
14. Schindler T, Bornmann W, Pellicena P, Miller WT, Clarkson B, Kuriyan J. Structural mechanism for STI-571 inhibition of abelson tyrosine kinase. Science 2000;289:1938–42.
15. Beissert T, Puccetti E, Bianchini A, Guller S, Boehrer S, Hoelzer D, Ottmann OG, Nervi C, Ruthardt M. Targeting of the N-terminal coiled coil oligomerization interface of BCR interferes with the transformation potential of BCR-ABL and increases sensitivity to STI571. Blood 2003;102:2985–93.
16. McWhirter JR, Galasso DL, Wang JY. A coiled-coil oligomerization domain of Bcr is essential for the transforming function of Bcr-Abl oncoproteins. Mol Cell Biol 1993;13:7587–95.
17. He Y, Wertheim JA, Xu L, Miller JP, Karnell FG, Choi JK, Ren R, Pear WS. The coiled-coil domain and Tyr177 of bcr are required to induce a murine chronic myelogenous leukemia-like disease by bcr/abl. Blood 2002;99:2957–68.
18. Zhang X, Subrahmanyam R, Wong R, Gross AW, Ren R. The NH(2)-terminal coiled-coil domain and tyrosine 177 play important roles in induction of a myeloproliferative disease in mice by Bcr-Abl. Mol Cell Biol 2001;21:840–53.
19. Zhao X, Ghaffari S, Lodish H, Malashkevich VN, Kim PS. Structure of the Bcr-Abl oncoprotein oligomerization domain. Nat Struct Biol 2002;9:117–20.
20. Smith KM, Yacobi R, Van Etten RA. Autoinhibition of Bcr-Abl through its SH3 domain. Mol Cell 2003;12:27–37.
21. Leslie NR, O'Prey J, Bartholomew C, Harrison PR. An activating mutation in the kit receptor abolishes the stroma requirement for growth of ELM erythroleukemia cells, but does not prevent their differentiation in response to erythropoietin. Blood 1998;92:4798–807.
22. Grignani F, Kinsella T, Mencarelli A, Valtieri M, Riganelli D, Lanfrancone L, Peschle C, Nolan GP, Pelicci PG. High-efficiency gene transfer and selection of human hematopoietic progenitor cells with a hybrid EBV/retroviral vector expressing the green fluorescence protein. Cancer Res 1998;58:14–19.
23. Zheng X, Beissert T, Kukoc-Zivojnov N, Puccetti E, Altschmied J, Strolz C, Boehrer S, Gul H, Schneider O, Ottmann OG, Hoelzer D, Henschler R, et al. Gamma-catenin contributes to leukemogenesis induced by AML-associated translocation products by increasing the self-renewal of very primitive progenitor cells. Blood 2004;103:3535–43.
24. Grez M, Becker S, Saulnier S, Knoss H, Ott MG, Maurer A, Dinauer MC, Hoelzer D, Seger R, Hossle JP. Gene therapy of chronic granulomatous disease. Bone Marrow Transplant 2000;25(Suppl 2):S99–S104.
25. Griswold IJ, MacPartlin M, Bumm T, Goss VL, O'Hare T, Lee KA, Corbin AS, Stoffregen EP, Smith C, Johnson K, Moseson EM, Wood LJ, et al. Kinase domain mutants of Bcr-Abl exhibit altered transformation potency, kinase activity, and substrate utilization, irrespective of sensitivity to imatinib. Mol Cell Biol 2006;26:6082–93.
26. Smith KM, Van Etten RA. Activation of c-Abl kinase activity and transformation by a chemical inducer of dimerization. J Biol Chem 2001;276:24372–9.
27. Puccetti E, Guller S, Orleth A, Bruggenolte N, Hoelzer D, Ottmann OG, Ruthardt M. BCR-ABL mediates arsenic trioxide-induced apoptosis independently of its aberrant kinase activity. Cancer Res 2000;60:3409–13.
28. O'Hare T, Walters DK, Stoffregen EP, Sherbenou DW, Heinrich MC, Deininger MW, Druker BJ. Combined Abl inhibitor therapy for minimizing drug resistance in chronic myeloid leukemia: Src/Abl inhibitors are compatible with imatinib. Clin Cancer Res 2005;11:6987–93.
29. O'Hare T, Walters DK, Stoffregen EP, Jia T, Manley PW, Mestan J, Cowan-Jacob SW, Lee FY, Heinrich MC, Deininger MW, Druker BJ. In vitro activity of Bcr-Abl inhibitors AMN107 and BMS-354825 against clinically relevant imatinib-resistant Abl kinase domain mutants. Cancer Res 2005;65:4500–5.
30. von Bubnoff N, Veach DR, van der Kuip H, Aulitzky WE, Sanger J, Seipel P, Bornmann WG, Peschel C, Clarkson B, Duyster J. A cell-based screen for resistance of Bcr-Abl-positive leukemia identifies the mutation pattern for PD166326, an alternative Abl kinase inhibitor. Blood 2005;105:1652–9.
31. Hantschel O, Superti-Furga G. Regulation of the c-Abl and Bcr-Abl tyrosine kinases. Nat Rev Mol Cell Biol 2004;5:33–44.
32. Skaggs BJ, Gorre ME, Ryvkin A, Burgess MR, Xie Y, Han Y, Komisopoulou E, Brown LM, Loo JA, Landaw EM, Sawyers CL, Graeber TG. Phosphorylation of the ATP-binding loop directs oncogenicity of drug-resistant BCR-ABL mutants. Proc Natl Acad Sci USA 2006;103:19466–71.